DEUTERON PHOTODISINTEGRATION USING QUASICONTINUUM OF P-WAVES IN CORRELATED GAUSSIAN BASIS

(Deuteronens fotodisintegration med kvasikontinuum af p-bølger i Gaussisk basis)

Denmark, September 2014

Bachelor's Thesis
submitted by

Alex Arash Sand Kalaee
Stud. no.: 20112369
Department of Physics and Astronomy,
Aarhus University

Supervised by

Dmitri Vladimir Fedorov

Abstract

In this thesis we will investigate whether the free particle state and photodisintegration of nuclei can be described using bound wave functions in an oscillator trap expanded into quasicontinuum. We will consider the photodisintegration of the deuteron, $d\gamma \to pn$, and estimate the total cross section in the dipole approximation.

For the p-wave basis we multiply a vector operator rather than the spherical harmonic functions to achieve pure p-wave states. The deuteron ground state and excited p-wave states are approximated using the stochastic variational method and the Hylleraas-Undheim-McDonald theorem on a basis of correlated Gaussian functions. To acquire continuum behaviour the system is placed in an oscillator trap expanded into quasicontinuum.

We have developed a variant of the correlated Gaussian method with explicit p-wave Gaussians and derived the necessary analytic expressions for the matrix elements. Our p-wave Gaussian basis was tested on the p-wave spectrum of hydrogen.

Further, we have derived the necessary formulae for calculation of the deuteron photodisintegration cross section using the wave-functions of the quasicontinuum of the correlated Gaussian method. Numerical approximation of the deuteron ground state and quasicontinuum successfully reproduced the cross section expected from experiments with deuteron photodisintegration. Our method thus has the potential to be applicable to more complicated quantum systems and reactions involving continuum states.

A first attempt at including spin-orbit forces in the model did, however, slightly diminish rather than increase the agreement with experiment. Further work is required to improve our model of the deuteron.

Contents

Chapter 1

Introduction

Ever since their discovery atomic nuclei have been subject to extensive studies of their physical properties. One fundamental characteristic of nuclei is the cross section of photodisintegration, the process of absorption of intense gamma radiation and ensuing decay by emission of subatomic particles. A theoretical description of photodisintegration requires knowledge of the wave function of the final state of free particles. Unfortunately the wave function of free particles grows increasingly difficult to write for higher numbers of particles. In this thesis we will investigate whether we can circumvent this problem by placing the system in a harmonic oscillator and only consider the bound states as the width of the oscillator is increased till the wave function exhibits continuum-like behaviour, i.e. a quasicontinuum.

As the deuteron is the simplest possible nucleon system, experimental and theoretical studies of it are numerous and extensive. Hence it is a reliable starting point for evaluating new methods and techniques. We will consider the deuteron and its absorption of gamma radiation, $d\gamma \rightarrow pn$. However, we assume that the photon, by transfer of angular momentum, excites the deuteron from the ground state s-wave to a p-wave state rather than a free particle state.

To acquire knowledge of the wave function of both the ground and final states we will assume the potential between the proton and neutron can be described by an operator with the radial parts of Gaussian functions. We estimate the wave function of these states using stochastic variational analysis on a correlated Gaussian basis to minimise the energies. As we wish to only consider excitations to p-wave states, we develop a p-wave basis by multiplying the Gaussian functions with prefactors of vector operators.

In this thesis we will initially introduce the deuteron and make first attempts at estimating the cross section using the zero-range approximation and the plane wave function, subsequently we will explain the theory and numerical methods employed in our oscillator model. We will next use the hydrogen system to evaluate the efficacy of our p-wave basis. Finally the results of our quasicontinuum are presented and discussed.

Chapter 2

The deuteron system

For the convenience of the reader we will here collect some basic information about the lightest compound nucleus – the deuteron.

The deuteron consists of a proton and a neutron. As the proton and neutron are particles with similar characteristics, they can be viewed as two different isospin states of the same particle, the nucleon [1, p. 14-17]. In this thesis we disregard the mass difference between the proton and neutron. Together the particles form an isospin doublet,

$$I = \frac{1}{2}: \quad \begin{cases} |\frac{1}{2}, \frac{1}{2}\rangle = |p\rangle \\ |\frac{1}{2}, -\frac{1}{2}\rangle = |n\rangle \end{cases} . \tag{2.1}$$

We wish to describe a two-nucleon system. The possible isospin configurations are the antisymmetric singlet state

$$I = 0: \quad \frac{1}{\sqrt{2}} \left(|pn\rangle - |np\rangle \right), \tag{2.2}$$

and the symmetric triplet states

$$I = 1: \quad \begin{cases} |pp\rangle \\ \frac{1}{\sqrt{2}} \left(|pn\rangle + |np\rangle \right) \\ |nn\rangle \end{cases} . \tag{2.3}$$

The singlet state describes a system of one proton and one neutron, i.e. a deuteron, and the triplet states describe three systems: a deuterium nucleus, a two-proton nucleus and a two-neutron nucleus. As the triplet states are degenerate states of two-nucleon nuclei, and we know that two-proton and two-neutron nuclei are not stable, the triplet deuteron describes a highly excited state. To form a deuteron ground state we must use the singlet isospin wave function.

As the nucleon is a spin-$\frac{1}{2}$ particle we require the total wave function of the two-nucleon system to be antisymmetric. The ground state spatial wave function is the symmetric s-wave. Thus to preserve antisymmetry of the total wave function, the spin wave function must be of the symmetric spin triplet state, $S = 1$. If we denote the total angular momentum J and the angular momentum states ${}^{2S+1}L_J$, we expect the ground state to be in the state ${}^3S_1$

which is of positive parity. As states of same total angular momentum and parity are able to mix [2, p. 103], we expect an admixture of the state ${}^3D_1$. The ground state of the deuteron has the energy $E_0 = -2.224575(9)$ MeV, root-mean-square radius $r_d = 1.971(6)$ fm and the d-state probability is 4-6% [3]. We will, however, assume the d-state admixture to be negligible. Due to the low binding energy no excited bound states of the deuteron exists. Additionally the isospin triplet state corresponds to the virtual spin singlet with an energy of about 60 keV [4].

Chapter 3

Deuteron photodisintegration in the zero-range approximation

In this chapter we shall reproduce the basic notation and formulae for the theory of deuteron photodisintegration using the zero-range approximation for the deuteron. The analysis is based on Taasti and Nielsen [5].

We will first introduce the initial and final states of the system and proceed to analyse the effect of quantum radiation in the dipole approximation. From this the differential cross section is found and finally the total cross section is obtained by spherical integration.

In the zero-range approximation we assume that the interaction between the nucleons can be described using a three-dimensional delta function potential. This potential has a single bound state,

$$\psi_0 = \sqrt{\frac{\kappa}{2\pi}} \frac{e^{-\kappa r}}{r}, \tag{3.1}$$

where r is the distance between the nucleons and κ is defined

$$\kappa = \frac{\sqrt{2\mu E_0}}{\hbar}. \tag{3.2}$$

Neglecting the interaction between the nucleons in the final state, we here apply the plane wave function,

$$\psi_f = \frac{1}{\sqrt{V}} e^{-\frac{i}{\hbar}\mathbf{pr}}. \tag{3.3}$$

Prior to interaction between deuteron and photon, we write the initial state of the system as

$$|\Psi_i\rangle = |\psi_0\rangle |1_{\mathbf{k}\lambda}\rangle \tag{3.4}$$

where $|\psi_0\rangle$ is our zero-range wave function and $|1_{\mathbf{k}\lambda}\rangle$ the single photon wave function with momentum $\mathbf{k}$ and polarisation λ. The final state of the system is

$$|\Psi_f\rangle = |\psi_f\rangle |0\rangle, \tag{3.5}$$

where $|\psi_f\rangle$ is the plane wave function and $|0\rangle$ the electromagnetic vacuum state.

3.1 Quantum radiation in the dipole approximation

During photodisintegration a free photon interacts with the deuteron. We consider this interaction in the dipole approximation where the interaction operator is given

$$\hat{V} = -\hat{\mathbf{d}}\hat{\mathbf{E}}(\mathbf{0}), \tag{3.6}$$

$\hat{\mathbf{d}}$ being the dipole moment operator and $\hat{\mathbf{E}}(\mathbf{r})$ the electric field.

We consider the electromagnetic field in the Coulomb gauge, thus the vector potential and scalar potential satisfies

$$\nabla\mathbf{A} = 0, \quad \phi = 0.$$

The electric field is given

$$\hat{\mathbf{E}} = -\frac{1}{c}\frac{\partial}{\partial t}\hat{\mathbf{A}} = -\frac{i}{\hbar c}\left[\hat{H}, \hat{\mathbf{A}}\right], \tag{3.7}$$

where

$$\hat{H} = \sum_{\mathbf{k}\lambda} \hbar\omega_{\mathbf{k}} \hat{a}^{\dagger}_{\mathbf{k}\lambda}\hat{a}_{\mathbf{k}\lambda} \tag{3.8}$$

is the Hamiltonian and

$$\hat{\mathbf{A}}(\mathbf{r}) = \sum_{\mathbf{k}\lambda} \sqrt{\frac{2\pi\hbar c^2}{\omega_{\mathbf{k}} V}} \left(\mathbf{e}_{\mathbf{k}\lambda}\hat{a}_{\mathbf{k}\lambda}e^{i\mathbf{kr}} + \mathbf{e}^{*}_{\mathbf{k}\lambda}\hat{a}^{\dagger}_{\mathbf{k}\lambda}e^{-i\mathbf{kr}}\right) \tag{3.9}$$

the vector potential. Here c is the speed of light, $\hat{a}_{\mathbf{k}\lambda}$ and $\hat{a}^{\dagger}_{\mathbf{k}\lambda}$ are, respectively, the annihilation and generation operators of a photon for which the following applies: momentum $c\mathbf{k}$, frequency $\omega_{\mathbf{k}} = ck$ and polarisation unit vector $\mathbf{e}_{\mathbf{k}\lambda}$ which is transverse: $\mathbf{e}^2 = 1$ and $\mathbf{k}\mathbf{e}_{\mathbf{k}\lambda} = 0$. The operators $\hat{a}_{\mathbf{k}\lambda}$ and $\hat{a}^{\dagger}_{\mathbf{k}\lambda}$ satisfy the bosonic commutation relations,

$$[\hat{a}_{\mathbf{k}\lambda}, \hat{a}^{\dagger}_{\mathbf{k}\lambda}] = \delta_{\lambda\lambda'}\delta_{\mathbf{k}\mathbf{k}'}. \tag{3.10}$$

Using (3.8) and (3.9) the electric field in the dipole approximation can be reduced to

$$\hat{\mathbf{E}}(\mathbf{0}) = i\sum_{\mathbf{k}\lambda} \sqrt{\frac{2\pi\hbar\omega_{\mathbf{k}}}{V}} \left(\hat{a}_{\mathbf{k}\lambda}\mathbf{e}_{\mathbf{k}\lambda} - \hat{a}^{\dagger}_{\mathbf{k}\lambda}\mathbf{e}^{*}_{\mathbf{k}\lambda}\right). \tag{3.11}$$

We consider the quantum system of a deuteron in relative coordinates between the neutron and the proton, thus the dipole moment operator is given as

$$\hat{\mathbf{d}} = 0 \cdot \mathbf{r}_n + e \cdot \mathbf{r}_p = \frac{e}{2}\mathbf{r}, \tag{3.12}$$

where e is the elementary charge.

3.2 The differential cross section

To find the cross section we are interested in the interaction strength, $|V_{fi}|^2$,

$$\begin{aligned} V_{fi} &= \langle\Psi_f|\hat{V}|\Psi_i\rangle \\ &= -\langle 0|\langle\varphi_p|\hat{\mathbf{d}}\hat{\mathbf{E}}(0)|\varphi_s\rangle|1_{\mathbf{k}\lambda}\rangle \\ &= ie\sqrt{\frac{2\pi\hbar\omega_{\mathbf{k}}}{V}}\mathbf{e}^{*}_{\mathbf{k}\lambda}\mathbf{d}_{fi}, \end{aligned} \tag{3.13}$$

where

$$\begin{aligned}\mathbf{d}_{fi} &= \langle\psi_f|\mathbf{r}_p|\psi_0\rangle \\ &= \int_V d^3r \frac{1}{\sqrt{V}} e^{-\frac{i}{\hbar}\mathbf{pr}} \frac{\mathbf{r}}{2}\sqrt{\frac{\kappa}{2\pi}}\frac{e^{-\kappa r}}{r} \\ &= \frac{2}{i\hbar}\sqrt{\frac{2\pi\kappa}{V}}\frac{1}{\left(\kappa^2+\frac{p^2}{\hbar^2}\right)^2}\mathbf{p}. \end{aligned} \tag{3.14}$$

To account for unpolarised light we average $|V_{fi}|^2$ over the two polarisations of the photon, $\lambda = 1, 2$

$$\begin{aligned}\frac{1}{2}\sum_{\lambda=1,2}|V_{fi}|^2 &= \frac{2e^2\pi\hbar\omega_{\mathbf{k}}}{V}\frac{1}{2}\sum_{\lambda=1,2}|\mathbf{e}^*_{\mathbf{k}\lambda}\mathbf{d}_{fi}|^2 \\ &= \frac{e^2\pi\hbar\omega_{\mathbf{k}}}{V}|\mathbf{d}_{fi}|^2\sin^2\theta \end{aligned} \tag{3.15}$$

where θ is the angle between $\mathbf{k}$ and $\mathbf{d}_{fi}$.

For a free particle we define the density of states after Gasiorowicz [6, p. 351]

$$d\nu = \frac{V}{(2\pi\hbar)^3}\int\delta\left(\hbar\omega_{\mathbf{k}} - E_0 - \frac{p^2}{2\mu}\right)d^3p. \tag{3.16}$$

The delta function can be rewritten using Gasiorowicz [6, p. 431]

$$\delta\left(f(x)\right) = \sum_j \frac{\delta(x-x_j)}{|\frac{df}{dx}|_{x=x_j}}, \tag{3.17}$$

where $f(x)$ is a general function and x_j, $j = 0, 1, 2, ...$, are the zeroes of $f(x)$.

In our case $f(p) = \hbar\omega_{\mathbf{k}} - E_0 - \frac{p^2}{2\mu}$, the zero of which is

$$p_0 = \sqrt{2\mu\left(\hbar\omega_{\mathbf{k}} - E_0\right)}, \tag{3.18}$$

as we require the norm of the momentum vector to be positive.

Thus the density of states for a solid angle, $d\Omega_{\mathbf{p}}$, in the direction of $\mathbf{p}$ is

$$d\nu = \frac{\mu p_0 V}{(2\pi\hbar)^3}d\Omega_{\mathbf{p}}. \tag{3.19}$$

Let dw be the probability per unit time of a photon taking part in photodisintegration, and from Fermi's golden rule we have

$$dw = \frac{2\pi}{\hbar}|V_{fi}|^2 d\nu, \tag{3.20}$$

where $d\nu$ is the density of final states [7, p. 125]. The differential cross section is related to the transition probability through

$$d\sigma = \frac{dw}{j}, \tag{3.21}$$

with $j = \frac{1}{V}c$ being the flux density of photons. Thus

$$d\sigma = \frac{V}{c}\frac{2\pi}{\hbar}|V_{fi}|^2\frac{\mu p_0 V}{(2\pi\hbar)^3}d\Omega_{\mathbf{p}}. \tag{3.22}$$

We now make the substitution $|V_{fi}|^2 \to \frac{1}{2}\sum_{\lambda=1,2}|V_{fi}|^2$, insert (3.14) and obtain

$$\begin{aligned} d\sigma &= \frac{\hbar\omega_{\mathbf{k}}\mu p_0 V}{4\hbar^3\pi}\frac{e^2}{\hbar c}|\mathbf{d}_{fi}|^2\sin^2\theta d\Omega_{\mathbf{p}} \\ &= 2\alpha\hbar\omega_{\mathbf{k}}\frac{\kappa}{\left(\kappa^2+\frac{p_0^2}{\hbar^2}\right)^4}\frac{p_0^3}{\hbar^3}\frac{\mu c^2}{(\hbar c)^2}\sin^2\theta d\Omega_{\mathbf{p}} \end{aligned} \tag{3.23}$$

where $\alpha = \frac{e^2}{\hbar c}$ is the fine structure constant.

3.3 The total cross section

To acquire the total cross section we integrate over all directions of $\mathbf{p}$,

$$\begin{aligned} \sigma &= 2\alpha\hbar\omega_{\mathbf{k}}\frac{\kappa}{\left(\kappa^2+\frac{p_0^2}{\hbar^2}\right)^4}\frac{p_0^3}{\hbar^3}\frac{\mu c^2}{(\hbar c)^2}\int\sin^2\theta d\Omega_{\mathbf{p}} \\ &= 2\alpha\hbar\omega_{\mathbf{k}}\frac{\kappa}{\left(\kappa^2+\frac{p_0^2}{\hbar^2}\right)^4}\frac{p_0^3}{\hbar^3}\frac{\mu c^2}{(\hbar c)^2}\int_0^{2\pi}d\phi\int_0^{\pi}\sin^3\theta d\theta \\ &= \frac{16\pi}{3}\alpha\hbar\omega_{\mathbf{k}}\frac{\kappa}{\left(\kappa^2+\frac{p_0^2}{\hbar^2}\right)^4}\frac{p_0^3}{\hbar^3}\frac{\mu c^2}{(\hbar c)^2}. \end{aligned} \tag{3.24}$$

We insert p_0 and κ in (3.24),

$$\sigma = \frac{16\pi}{3}\alpha\hbar\omega_{\mathbf{k}}\frac{\sqrt{2\mu E_0}}{\hbar\left(\frac{2\mu E_0}{\hbar^2}+\frac{2\mu(\hbar\omega_{\mathbf{k}}-E_0)}{\hbar^2}\right)^4}\frac{[2\mu(\hbar\omega_{\mathbf{k}}-E_0)]^{3/2}}{\hbar^3}\frac{\mu c^2}{(\hbar c)^2}, \tag{3.25}$$

which reduces to

$$\sigma = \frac{4\pi}{3}\alpha\sqrt{\epsilon_0}\frac{(\hbar c)^2}{\mu c^2}\frac{(E_\gamma - E_0)^{3/2}}{E_\gamma^3}, \tag{3.26}$$

where $E_\gamma = \hbar\omega_{\mathbf{k}}$ is the photon energy.

In Figure 3.1 the estimated cross section is compared to experimental data from Rozpedzik et al. [8]. We notice that our results from the zero-range approximation agree in shape with experiment but is a factor 5/3 too low. One shortcoming of our analysis is the zero-range approximation; the real range of the inter-nucleon potential in the deuteron is finite, albeit short. Additionally the plane wave approximation is difficult to write for systems of arbitrary number of particles. These shortcomings are evaded by regarding the particles in a quasicontinuum of bound p-wave states. This approach will be covered in the next chapter.

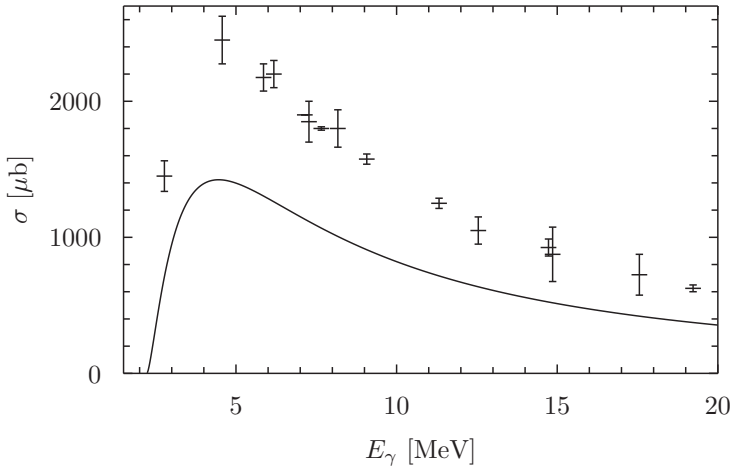

Figure 3.1: *Estimated total cross section for photodisintegration from the zero-range approximation, experimental data is from Rozpedzik et al. [8, Fig. 3].*

Chapter 4

Deuteron photodisintegration in correlated Gaussian method

In chapter 3 we found the zero-range approximation inadequate to describe the bound state of the deuteron. In addition, the plane wave function grows increasingly more difficult to write for systems of higher numbers of particles. In this chapter we shall introduce the correlated Gaussian method of explicit p-wave Gaussians and derive the photodisintegration formulae for the quasi-continuum spectrum of this method.

In order to achieve this we first describe the internucleon force present in the ground state, and the force and orbital angular momentum state present in the excited state. As we mean to employ the Hylleraas-Undheim-McDonald theorem to approximate the true wave function of the ground and excited states, we next introduce the generalised eigenvalue problem followed by our method of optimisation. The quality of the approximation depends on the choice of basis. In this thesis we employ the correlated Gaussian basis. Our next step is therefore to describe the ground state and develop a variant for the p-wave states, using the correlated Gaussian basis. Subsequently we introduce the unit systems and method of parameter estimation applied in the numerical analysis. Finally we determine the cross section in the quasicontinuum followed by the numerical estimate of the cross section.

The finite range of the two-nucleon potential has previously been successfully described using operators with radial shapes of Gaussians [9, 3]. Assuming that the deuteron ground state can de adequatly described by a central potential of the form,

$$\hat{V_c} = V_c \exp\left\{-\frac{r^2}{b_c^2}\right\}, \tag{4.1}$$

where V_c and b_c are the strength and radius of the central potential, respectively, we can approximate the wavefunction for this potential using a basis of correlated Gaussian functions, see section 4.3, which we choose to serve as our wave function for the inital state.

To consider the final state we now redefine the problem. Rather than consider transitions to states of free, unbound particles, we assume that the photon, due to transfer of its single quantum of angular momentum, excites the deuteron to a p-wave state

$$^3\mathrm{S}_1 \rightarrow {}^3\mathrm{P}_\mathrm{J}, \tag{4.2}$$

where $J = 0, 1, 2$ and the spin triplet state is conserved in the dipole approximation. Similarly to the initial state we will use a basis of correlated Gaussian functions to approximate the wave function of the final state.

Due to the rapid asymptotic behaviour of Gaussian functions the basis is widely used to describe wave functions of bound states. Their strength, however, renders them inadequate at approximating the continuum spectrum. We assume that in the p-wave the nucleons experience a harmonic oscillator potential with bound eigenstates. If we increase the width of the oscillator sufficiently the eigenstates approach a quasicontinuum where we expect the system to exhibit continuum behaviour.

4.1 The generalized eigenvalue problem

To study the deuteron system we need to estimate the eigenstates and corresponding eigenenergies of its Hamiltonian, $\hat{H}$. For a given eigenstate we know from the time-independent Schrödinger equation,

$$\hat{H}|\Psi\rangle = E|\Psi\rangle, \tag{4.3}$$

where $|\Psi\rangle$ is a true eigenstate of the Hamiltonian with eigenenergy E. Let us now consider an arbitrary trial wave function, $|\varphi_k\rangle$, from our subspace of basis functions, and insert it into our eigenvalue equation,

$$\hat{H}|\varphi_k\rangle = \epsilon_k|\varphi_k\rangle, \tag{4.4}$$

ϵ_k is the energy corresponding to the state $|\varphi_k\rangle$. As the trial wave function lies in our subspace of basis functions, $|\phi_i\rangle$, we can write it as

$$|\varphi_k\rangle = \sum_{i=1}^{N} c_i|\phi_i\rangle, \tag{4.5}$$

with N being the number of basis functions and c_i complex scalars. The eigenvalue equation can thus be rewritten as

$$\hat{H}\sum_{i=1}^{N} c_i|\phi_i\rangle = \epsilon_k \sum_{i=1}^{N} c_i|\phi_i\rangle. \tag{4.6}$$

Taking the inner product on both sides with $\langle\varphi_k|$ restates the equation in the form

$$\mathcal{H}\mathbf{c} = \epsilon_k\mathcal{N}\mathbf{c}, \tag{4.7}$$

where $\mathbf{c}$ is a vector of the c_i-coefficients and $\mathcal{H}$, $\mathcal{N}$ are the Hamiltonian and overlap matrices respectively, with entries

$$\mathcal{H}_{(i,j)} = \langle\phi_i|\hat{H}|\phi_j\rangle, \quad \mathcal{N}_{(i,j)} = \langle\phi_i|\phi_j\rangle. \tag{4.8}$$

Note that the basis functions are not orthogonal and $\mathcal{N}$ is thus *not* simply proportional to the identity matrix.

This system is known as the generalized eigenvalue problem. According to the Hylleraas-Undheim-McDonald theorem [10, p. 696] the kth lowest eigenenergy, ϵ_k, is an upper bound to the kth lowest true eigenenergy, E_k. Hence

adjusting the parameters of $|\phi_i\rangle$ to minimise the eigenenergies, one's estimate of the eigenenergies usually converges close to the true values. Our strategy is to approximate the true wave function by minimising the eigenenergy of the trial wave function. A reliable technique is the stochastic variational method. The quality of the approximation is improved by repeatedly suggesting new random parameters to the basis functions, determining their expectation values and preserving those who improve upon one's results. In the case of minimising the expected energy, the stochastic technique reduces the risk of settling in local minima compared to other minimisation techniques, simply by suggesting parameters independently of those already in use. In the next section we describe how we determine the eigenenergy and perform the optimisation.

4.2 Eigenenergies and optimisation

In section 4.1 we showed that the eigenvalue equation reduces to the generalised eigenvalue problem

$$\mathcal{H}\mathbf{c} = \epsilon_k \mathcal{N}\mathbf{c}. \tag{4.9}$$

The GSL routine `gsl_eigen_genhermv` solves complex systems of the form (4.9) through Cholesky decomposition and returns both a vector of the eigenenergies and a matrix in which the kth column represents the coefficients $\mathbf{c}$ for the kth element of the eigenenergy vector.

Cholesky decomposition, however, requires the overlap matrix, $\mathcal{N}$, to be positive semi-definite [11]. Since $\mathcal{N}$ is an overlap matrix it is a Gramian matrix and thus positive semi-definite [12]. However, this is only the case if every possible pair of component functions of the total trial wave function are not too alike. We assure this by requiring that for each proposed set of parameters on the jth function the overlap is below a given threshold

$$\frac{\langle\varphi_j|\varphi_i\rangle}{\sqrt{\langle\varphi_i|\varphi_i\rangle\langle\varphi_j|\varphi_j\rangle}} < T \quad \text{for all } i \neq j. \tag{4.10}$$

If the overlap is above the threshold the component is discarded and another proposed. The proper threshold depends on the system in question, as it is a compromise between being sufficiently low to ensure positive semi-definiteness of $\mathcal{N}$ while high enough to allow a wide range of different components to the trial wave function.

To optimise the trial wave function we will use the method of iterative refinement. In this scheme we begin with a trial function of k components. To optimise the jth part we propose n new components stochastically. If replacing the jth function with any of these candidates improves, i.e. lowers, the lowest eigenenergy of the system then the old function is discarded and the new used instead. When the iteration is completed for $j = 1, \cdots, k$ the program has completed one loop. Let ϵ and ϵ' denote the lowest eigenvalues before and after a loop respectively. If the relative improvement is below a certain threshold,

$$\left|\frac{\epsilon' - \epsilon}{\epsilon}\right| < T_{\text{loop}}, \tag{4.11}$$

the program will assume that the true eigenfunction is well converged and that further, significant improvements are unlikely, wherefore the optimisation is halted. The threshold is set at $T_{\text{loop}} = 10^{-7}$.

The efficacy of the optimisation does, however, depend on one's choice of basis functions. We choose a basis of Gaussian functions in Cartesian coordinates, as will be described in the following section.

4.3 The correlated Gaussian basis

The last two decades have seen a great increase in the use of Gaussians to approximate quantum states; from numerical analysis in quantum chemistry to studies of the hydrogen atoms, the Gaussian basis has proven useful and accurate. A basis of Gaussian functions has the benefit of relatively easy separation of the function in each Cartesian coordinate and the likewise simple differentiation and integration of the functions, allowing many matrix elements to be computed analytically maintaining both precision and ease of computation thus making major optimisation attainable [10, p. 695-696]. For this reason we choose the correlated Gaussian basis for this thesis.

The three-dimensional Gaussian for an N-body system is given as

$$G(\mathbf{x}) = \exp\left\{-\mathbf{x}^T A \mathbf{x}\right\}, \tag{4.12}$$

in which $\mathbf{x} = (\mathbf{x}_0, \mathbf{x}_1, \ldots, \mathbf{x}_N)$ is a supervector of the Jacobi coordinates and A is a matrix of adjustable parameters. The argument is defined

$$\mathbf{x}^T A \mathbf{x} \equiv \sum_{(i,j)} A_{(i,j)} \mathbf{x}_j^T \mathbf{x}_i. \tag{4.13}$$

In our case we wish to describe the two-nucleon system of a deuteron. As none of the forces acting on the deuteron depend on their laboratory coordinates, only on the relative distance, the system can be reduced to that of a single particle of reduced mass $\mu = \frac{1}{2} m_p$. In this simplification the supervector and matrix are reduced respectively to a single distance vector, $\mathbf{r}$, and scalar parameter, A.

The Gaussian functions above are, however, spherically symmetric and hence alone only accounts for the s-wave states. Different approaches are possible within the Gaussian scheme to break spherical symmetry and accommodate non-zero angular momenta. One possible solution is that of shifted Gaussians,

$$\psi = \exp\left\{-A(\mathbf{r} - \mathbf{s})^2\right\}, \tag{4.14}$$

in which $\mathbf{s}$ is the adjustable shifting vector. While this approach accommodates multiple non-zero angular momentum states [13], it carries the drawback of our inability to predefine the desired angular momentum. Every trial function becomes a superposition of mixed angular momenta. One alternative is to use a basis of Gaussians prefactored with spherical harmonic functions

$$\psi = \theta_{l,m} \exp\left\{-Ar^2\right\}, \tag{4.15}$$

where $\theta_{l,m}$ is the spherical harmonic function for a given set of quantum numbers, orbital angular momentum, l, and magnetic quantum number, m. Spherical harmonics, however, are difficult to write in general, especially in Cartesian coordinates. We will use a different approach and replace the spherical harmonics with a vector operator on the position vector.

We are only concerned with the s- and p-wave states, and thus our s-wave basis is

$$\psi = \exp\left\{-Ar^2\right\}, \tag{4.16}$$

and the p-wave basis is

$$\psi = \mathbf{a}^T\mathbf{r}\exp\left\{-Ar^2\right\}. \tag{4.17}$$

The vector operator, $\mathbf{a}$, is a Cartesian vector of adjustable parameters.

If the system is subject to no external force its Hamiltonian is spherically symmetric and states of different magnetic quantum numbers in the p-wave will thus be three-fold degenerate. In such a case it will usually be sufficient to only consider the $m = 0$ states, and the parameter values of $\mathbf{a}$ can thus remain real. However, say we imposed an external field to the deuteron. The Hamiltonian would then be spherically non-symmetric, in turn requiring complex values in $\mathbf{a}$ to account for the resultant complex phase of the spherical harmonic functions with non-zero m.

The Gaussian basis is a linearly dependent basis. This is both a strength and weakness in the stochastic variational method. As the basis functions are linearly dependent, they are also non-orthogonal, which increases the necessary amount of calculations. However, linear dependence, by definition, ensures that one can express the same function through different linear superpositions of basis functions. We can thus hope to improve our trial function without needing to actively ensure completeness of the basis. Likewise different sessions can stochastically produce various sets of parameters, thus creating technically different trial functions, while still capable of approximating the true wave function equally well. Hence linear dependence of the basis increases the efficacy of the stochastic variational method.

Before moving on to determining the cross section from our quasicontinuum, we will define our unit system and describe how the parameters of the basis functions are selected.

4.4 Unit systems and estimation of the parameters

To make the numerical analysis more feasible we will introduce two different unit systems. In the deuteron system the convenient scales of length and length are the fm and MeV which we set to unity together with the reduced Planck constant in the nuclear units (n.u.)

$$1\text{ MeV} = 1\text{ fm} = \hbar = 1\text{ n.u.} \tag{4.18}$$

As a consequence the mass of a proton is $m_p = 0.02411$ n.u.

To evaluate our trial wave function for the p-wave state we will also analyse the hydrogen system. In this case the atomic units (a.u.) are more convenient. In the atomic units we set the reduced Planck constant, mass of the electron and the elementary charge to unity,

$$m_e = \hbar = e = 1\text{ a.u.} \tag{4.19}$$

Consequently the ground state energy of hydrogen satisfies $-2E_0 = 1$ a.u. $= 27.2$ eV, the Bohr radius is equal to unity, $a_o = 1$ a.u., and the unit of magnetic field is 1 a.u. $= 235$ kT [7, Table A14.2].

Each component of the trial function is characterised by a set of variational parameters. Although the parameters of the trial wave function is selected randomly, the range of possible values needs to be constrained to those which make physical sense.

For the s-wave trial function, the functions are spherical Gaussians with scalar parameter A, which determines the extent of the Gaussian,

$$\psi = \exp\left(-Ar^2\right), \quad A = \frac{1}{b^2}, \tag{4.20}$$

where b is the radius of the Gaussian. As the root-mean-square radius of the deuteron ground state is of the order about 2 fm we assume that Gaussians of radii from 0.1 to 30 fm are sufficient to describe the system in this state. To ensure a more uniform distribution of different orders of magnitude, we determine b from

$$b = 10^{\varsigma} \text{ n.u.} \Rightarrow A = 10^{-2\varsigma} \text{ n.u.}, \tag{4.21}$$

where ς is choosen from a uniform distribution on the interval [-1;1.5] using the GNU Scientific Library (GSL) routine `gsl_ran_flat`.

For the p-wave trial function,

$$\mathbf{a}^T\mathbf{r}\exp\left(-Ar^2\right), \tag{4.22}$$

we need Gaussians of higher widths to consider the excited states of the deuteron, likewise the narrow Gaussians are not necessary to complete our descriptions. Hence, we allow the p-wave Gaussians to carry radii from 1 fm to 100 fm, thus ς is chosen from a uniform distribution on the interval [0;2]. We will also consider the p-wave of hydrogen, in which case the relevant scaling is the Bohr radius, $a_0 = 1$ a.u. We assume that radii from $0.1a_0$ to $30a_0$ are sufficient and select ς from the interval [-1;1.5].

To construct the p-wave we also need a vector parameter $\mathbf{a}$ in cartesian coordinates. As every component of the trial function is given a scaling coefficient through the matrix decomposition, see section 4.2, the vector length need not be subject to variation. Likewise, to accomodate states of non-zero L_z values a complex phase is needed. However, this is also provided by the decomposition of the matrices and need not be included in the variation. Thus for each function we choose $\mathbf{a}$ as a unit vector pointing in a random direction with a uniform distribution along all directions. Any relevant scaling and complex phase is provided by the decomposition. The direction is chosen through the GSL routine `gsl_ran_dir_3d`.

We are now able to perform optimisation on the eigenvalues and approximate the initial and final states of deuteron photodisintegration, from which we can obtain the cross section.

4.5 Cross section in the quasicontinuum

In section 3.2 we acquired some useful results for the cross section in general. We will continue from some of these to estimate the cross section for the photodisintegration in our quasicontinuum.

The interaction strength averaged over different polarisations of the photon is

$$\frac{1}{2}\sum_{\lambda=1,2}|V_{fi}|^2 = \frac{e^2\pi\hbar\omega_{\mathbf{k}}}{V}|\mathbf{d}_{fi}|^2\sin^2\theta \tag{4.23}$$

where θ is the angle between $\mathbf{k}$ and $\mathbf{d}_{fi}$, and

$$\mathbf{d}_{fi} = \langle\varphi_f|\mathbf{r}_p|\varphi_i\rangle. \tag{4.24}$$

Integrating over all values of θ yields

$$\frac{1}{2}\sum_{\lambda=1,2}|V_{fi}|^2 = \frac{4e^2\pi\hbar\omega_{\mathbf{k}}}{3V}|\mathbf{d}_{fi}|^2. \tag{4.25}$$

Let dw be the probability per unit time of the photon taking part in photodisintegration, from Fermi's golden rule

$$dw = \frac{2\pi}{\hbar}|V_{fi}|^2 d\nu, \tag{4.26}$$

where $d\nu$ is the density of final states. The differential cross section is related to the transition probability through

$$d\sigma = \frac{dw}{j} \tag{4.27}$$

with $j = \frac{1}{V}c$ being the flux density of photons. If we make the substitution $|V_{fi}|^2 \to \frac{1}{2}\sum_{\lambda=1,2}|V_{fi}|^2$ we obtain

$$\begin{aligned} d\sigma &= \frac{8e^2\pi^2\hbar\omega_{\mathbf{k}}}{3\hbar c}|\mathbf{d}_{fi}|^2 d\nu \\ &= \frac{8}{3}\pi^2\alpha\hbar\omega_{\mathbf{k}}|\mathbf{d}_{fi}|d\nu, \end{aligned} \tag{4.28}$$

where $\alpha = \frac{e^2}{\hbar c}$ is the fine structure constant. Integrating over both sides yields

$$\sigma = \frac{8}{3}\pi^2\alpha\hbar\omega_{\mathbf{k}}|\mathbf{d}_{fi}|\nu. \tag{4.29}$$

To estimate the cross section we lastly need to determine the density of states from the energy spectrum retrieved via the generalised eigenvalue problem. In the next section we will consider how this is done.

4.6 Numerical estimates of the cross section

As the method of correlated Gaussians only describes discrete eigenenergies we expect a spectrum with the levels

$$\epsilon_0 \leq \epsilon_1 \leq \cdots \leq \epsilon_j \leq \cdots \leq \epsilon_{N-1}, \tag{4.30}$$

where N is the number of energy levels described by our model.

If we assume that the energy levels are nondegenerate we will describe the density of states at the jth level as

$$\nu(\epsilon_j) = \frac{2}{\epsilon_{j+1} - \epsilon_{j-1}}, \tag{4.31}$$

that is the reciprocal of the energy interval closer to ϵ_j than to ϵ_{j-1} or ϵ_{j+1}. Using (4.29) the cross section is estimated

$$\sigma(\epsilon_j) = \zeta_j \nu, \quad \zeta_j = \frac{8}{3}\pi^2 \alpha \hbar \omega_{\mathbf{k}} |\mathbf{d}_{f_j i}|, \tag{4.32}$$

where ζ_k stems from $|\varphi_k\rangle$, the trial wave function with the energy ϵ_k. Note that a state of energy ϵ_j corresponds to absorption of a photon of energy $E_\gamma = \epsilon_j - E_0$.

If the energies are degenerate, however, the above estimate would result in division by zero, or almost zero as the finite machine precision and incomplete representation in the basis states renders the levels not exactly identical. We assume that each level is n-fold degenerate. The jth level would then begin at ϵ_{jn} and end at $\epsilon_{(j+1)n-1}$. The energy of the jth level is now estimated to be

$$\bar{\epsilon}_j = \frac{1}{2}\left(\epsilon_{jn} + \epsilon_{(j+1)n-1}\right). \tag{4.33}$$

Despite the degeneracy we define $\nu(\bar{\epsilon}_j)$ as in (4.31),

$$\nu(\bar{\epsilon}_j) = \frac{2}{\bar{\epsilon}_{j+1} - \bar{\epsilon}_{j-1}}, \tag{4.34}$$

however, we make the substitution $\zeta_j \to \bar{\zeta}_j$ evaluated as

$$\bar{\zeta}_j = \sum_{k=jn}^{(j+1)n-1} \zeta_k. \tag{4.35}$$

Finally the cross section is estimated

$$\sigma(\bar{\epsilon}_j) = \bar{\zeta}_j \nu(\bar{\epsilon}_j). \tag{4.36}$$

Chapter 5

Testing the method: p-states of hydrogen atom and the Zeeman effect

To evaluate the quality of our p-wave basis functions we will first study the hydrogen atom. All relevant matrix elements are provided in Appendix A.

Neglecting fine structure, the electron in hydrogen experiences a potential from the Coulomb force alone, in atomic units,

$$V(r) = -\frac{1}{r}. \tag{5.1}$$

The Hamiltonian is thus

$$\hat{H} = -\frac{1}{2}\nabla^2 - \frac{1}{r}. \tag{5.2}$$

The analytical solution to the Hamiltonian yields the energies

$$E_n = \frac{E_1}{n^2} = -\frac{1}{2n^2} \text{ a.u.}, \tag{5.3}$$

where $n = 1, 2, \ldots$ is the energy level [14, p. 149]. In our system the Hamiltonian commutes with the L_z-operator. The energy eigenstates are thus also eigenstates of the L_z-operator with eigenvalues $m\hbar$. We notice that the Hamiltonian of our system is spherically symmetric, hence we expect the energy eigenstates to be degenerate. In the case of the p-wave we expect a three-fold degeneracy between the states $m = 0, \pm 1$.

As the p-wave states are allowed for $n \geq 2$ we expect that the first three states, the 2p states, are degenerate with energy $E_2 = -0.125$ a.u. We have run an instance of the program using 50 components in the trial function and 50 candidates per iteration, the threshold overlap was $T = 0.6$. Optimisation required nine loops to terminate. The results for the 2p states can be seen in Table 5.1, note that the highest deviation is of the order of 10^{-5}.Thus our basis is able to reproduce the energy spectrum of the degenerate states.

If we apply an external, static magnetic field to the system we expect a splitting of the energy levels due to difference in magnetic quantum number, m. This splitting is known as the Zeeman effect. As the interaction depends on the angular momentum, the capability of our prefactored Gaussian basis to

Table 5.1: *Results from calculations on the hydrogen atom for the 2p states.*

Quantity	Exp. value [a.u.]	Results [a.u.]	Rel. deviation
E	-0.125	-0.12500	$8 \cdot 10^{-9}$
		-0.12500	$9 \cdot 10^{-6}$
		-0.12500	$2 \cdot 10^{-5}$
L^2	2	2.0000	$-3 \cdot 10^{-14}$
		2.0000	$-5 \cdot 10^{-15}$
		2.0000	$-4 \cdot 10^{-14}$

replicate the Zeeman effect yields information about the capacity of the basis to approximate eigenstates of the L_z operator.

When we apply an external, static magnetic field, $\mathbf{B}$, to the system, we specify a preferred direction of space and break the spherical symmetry. The magnetic field interacts with the orbital angular momentum, $\mathbf{L}$, of the nucleons and the new Hamiltonian is no longer spherically symmetric. For convenience we define the z axis to point in the same direction as the magnetic field, the interaction thus only depends on the z-projection of the orbital angular momentum, L_z.

If the magnetic field is weak compared to the internucleon potential we can regard the effect of the field as a perturbation on the energy eigenstates. The perturbation contains two terms: one linear in field strength, the *paramagnetic* term, and one quadratic in field strength, the *diamagnetic* term [7, p. 289]. As most relevant magnetic fields are no stronger than a fraction of one tesla the diamagnetic term is negligible and we need only consider the paramagnetic term. In addition the paramagnetic term is proportional to the angular momentum, if we assume the nucleons are in a spin singlet state, hence the energy shift is to a good approximation proportional to L_z in the domain of weak magnetic fields. As L_z is linear in m we expect the energy shift to be proportional to both field strength and m.

The perturbation from the magnetic field is,

$$\hat{H}' = \frac{\mu_N}{\hbar} B \hat{L}_z, \tag{5.4}$$

where $\mu_N = \frac{e\hbar}{2m_p}$ is the nuclear magneton [7, p. 290].

Applying the simulation to our new Hamiltonian $\hat{H} + \hat{H}'$ for various field strengths yields the data in Figure 5.1 for the 2p and 3p states, and a single line of the 4p state.

We notice that the energies are all linear in field strength as expected, likewise the splitting is in three different lines as expected from the three-fold degeneracy.

To estimate the expectation values of the L_z-operator we note from (5.4) the relation

$$\langle L_z \rangle = \frac{\hbar \Delta E}{\mu_N \Delta B}. \tag{5.5}$$

As the energy shift is linear in field strength the slope $\frac{\Delta E}{\Delta B}$ and, correspondingly, the expectation value $\langle L_z \rangle$ are constant. The L_z-values estimated from (5.5) for the 2p states are given in Table 5.2.

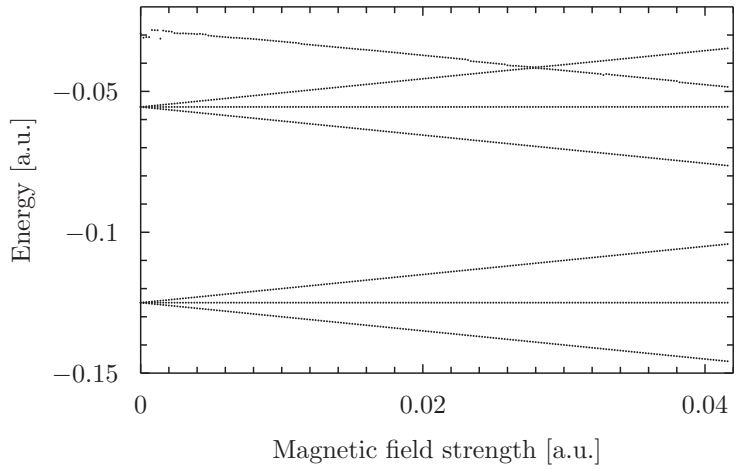

Figure 5.1: *Energy spectrum for the lowest eigenstates of the Hamiltonian with perturbation* (5.4).

Table 5.2: *Estimation of L_z-values for the 2p states from the slope of the energies.*

Quantity	Exp. value [a.u.]	Estimate [a.u.]	Rel. deviation
L_z	1	1.0000	$7 \cdot 10^{-16}$
	0	$-2.4 \cdot 10^{-6}$	–
	-1	-1.0000	$5 \cdot 10^{-6}$

From our analysis above we see that the trial functions of (4.17) are able to reproduce the expected energies of the hydrogen atom and expectation values of the angular momentum operator. Likewise the functions exhibit the behaviour expected from applying an external magnetic field to the system. Hence the trial functions are sufficient to describe a p-wave state.

Chapter 6

Results

In the following chapter the estimated eigenenergies for different Hamiltonians and the resulting cross section are given. All matrix elements used in the program to calculate a given system are provided in Appendix A.

6.1 The deuteron ground state and oscillator trap

To approximate the ground state of the deuteron we assumed in Chapter 4 that the internucleon potential is sufficiently described by a central field the shape of a Gaussian,

$$\hat{V}_c = V_c \exp\left\{-\frac{r^2}{b_c^2}\right\}, \tag{6.1}$$

where V_c and b_c are the strength and radius of the potential respectively.

To obtain suitable parameters of the potential the strength and radius were adjusted to reproduce the experimental data, r_d and E_0, for the ground state. We found that the parameters

$$V_c = -61.4858 \text{ MeV}, \quad b_c = 1.635 \text{ fm}, \tag{6.2}$$

reproduced the desired ground state. Using a trial function of 20 components and 40 candidates per iteration, the overlap threshold was set at $T = 0.98$. Optimisation was terminated after five loops. The ground state energy and root-mean-square radius are given in Table 6.1. The trial function describing this state will serve as our deuteron ground state wave function for the remainder of this thesis.

Table 6.1: *Estimate of the ground state energy and root-mean-square radius in a potential with the parameters of* (6.2).

Quantity	Deuteron	Gaussian model
E_0 [MeV]	-2.224575(9)	-2.224575
r_d [fm]	1.971(6)	1.970

As an approximation of the exited state, we assume that the nucleons only experience the harmonic oscillator potential,

$$V_{\text{osc.}} = \frac{1}{2}kr^2, \tag{6.3}$$

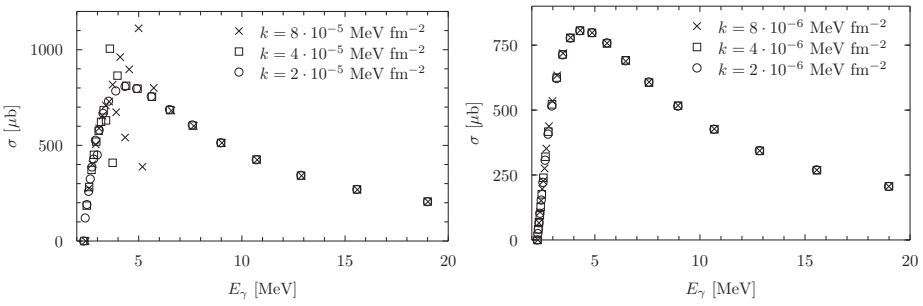

(a) Narrow oscillator trap (b) Wide oscillator trap

Figure 6.1: Convergence of cross section during expansion of the oscillator trap.

where k describes the width of the potential.

Further, to reduce the number of necessary components in the trial functions we only consider transitions to states with $L_z = 0$. The vectors $\mathbf{a}$ of the p-wave functions are all set to point in the positive z direction,

$$\mathbf{a} = \mathbf{e}_z. \tag{6.4}$$

For a given k the energy spectrum is found. Our program uses a trial function of 40 components and 40 candidates per iteration. The threshold of the overlap is set as $T = 0.991$. From the acquired spectrum the density of states and cross section is found using nondegenerate analysis, see section 4.6. We expand the oscillator trap till the cross section is converged, see Figure 6.1. The cross section is well converged for an oscillator potential where $k = 8 \cdot 10^{-6} \frac{\text{MeV}}{\text{fm}^2}$.

We now wish to evaluate our current results. The retrieved cross section is multiplied by 3 to account for the three-fold degeneracy of the true eigenstates. Further, we use spline interpolation to acquire an estimate for the cross section between the retrieved points. The total cross section of the first approximation is given in Figure 6.2. Experimental data are the same as in Figure 3.1. The dotted line represents estimates made by Rozpedzik et al. [8, Fig. 3] based on contributions from the single nucleon current and one pion exchange.

We note that our results agree considerably better with experiment than results from the zero-range approximation. In the low-energy region, below 6 MeV, our prediction slightly underestimates the cross section. As contribution from the magnetic dipole interaction is noticeable in the low-energy region [15], the discrepancy is possibly due to the dipole approximation. Our model does not account for contribution from higher orders of electromagnetic interaction. In addition our model does not account for d-state admixture in the ground state. As the admixture is 4-6% this could affect the final estimate of the total cross section. Likewise our present model does not include spin interactions in the excited states, this would also affect the final estimate of the total cross section. Since we do not know how spin will influence the final estimate, we will explore this further in the next section.

When we compare the results to the prediction from Rozpedzik et al. [8] we note that their prediction agrees better with the experimental data in the low-energy region. Between 6 MeV and 10 MeV the prediction from our model and the prediction from Rozpedzik et al. both follow experimental data equally

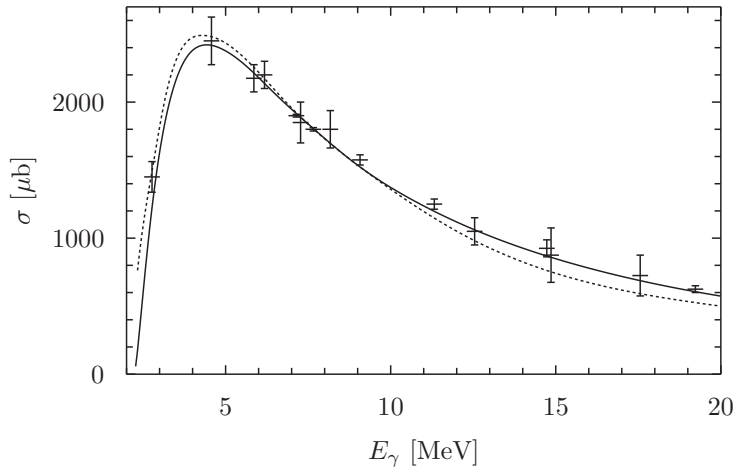

Figure 6.2: *Total cross section from our first approximation (solid line), experimental data are the same as in* Figure 3.1. *The dotted line represents estimates made by Rozpedzik et al.* [8, Fig. 3].

well. However, at higher energies above 10 MeV, our prediction agrees better with the experiment. Hence our model is equally valid to describe the total cross section of photodisintegration of the deuteron.

In this section we have shown that the method of correlated Gaussian functions in a quasicontinuum is sufficient to calculate the total cross section of photodisintegration of the deuteron. Hence the correlated Gaussian method has the potential to be applicable to the domain of quantum reactions and systems involving continuum states – a domain where this method has hitherto not been used. In the next section we will investigate whether the inclusion of spin will improve our model.

6.2 Effects of spin on the photodisintegration

Finally, we wish to include the central potential and spin in our model. The deuteron has four possible spin states, χ,

$$|\uparrow\uparrow\rangle, \quad |\downarrow\downarrow\rangle, \quad \frac{1}{\sqrt{2}}\left(|\uparrow\downarrow\rangle + |\downarrow\uparrow\rangle\right), \quad \frac{1}{\sqrt{2}}\left(|\uparrow\downarrow\rangle - |\downarrow\uparrow\rangle\right), \tag{6.5}$$

which satisfy the ordinary ortonormal relations. The program will assign each of the components of the trial function a random spin state.

The estimated central potential of the ground state compensated for d-state admixture and the resulting spin-orbit, spin-spin and tensor forces. The spin-orbit and tensor force are different in the p-wave, however. For the p-wave potential we use the potential from Garrido, Fedorov and Jensen [9], where we have assumed the tensor force to be negligible. The nucleon-nucleon potential is then

$$V_{nn} = \left(V_c + V_{ss}\mathbf{s}_1 \cdot \mathbf{s}_2 + V_{\mathrm{so}}\hat{\mathbf{L}} \cdot \hat{\mathbf{S}}\right) \exp\left\{-\frac{r^2}{b_{nn}^2}\right\}, \tag{6.6}$$

which includes central, spin-spin and spin-orbit forces. The operators $\mathbf{s}_1$ and $\mathbf{s}_2$ are the spins of the two nucleons and $\hat{\mathbf{S}} = \mathbf{s}_1 + \mathbf{s}_2$ the two-particle spin-operator. The parameters of this potential are given as

$$\begin{aligned} V_c &= -2.92 \text{ MeV}, \quad V_{ss} = -45.22 \text{ MeV} \\ V_{\text{so}} &= 12.08 \text{ MeV}, \quad b_{nn} = 1.8 \text{ fm}. \end{aligned} \tag{6.7}$$

In addition the system is again subject to the oscillator potential $V_{\text{osc.}}$ from section 6.1.

As we study the photodisintegration in the dipole approximation the spin-states remain untouched, hence the element $\mathbf{d}_{fi}$ is redefined to allow only components of the same spin state as the ground state, $|\chi_i\rangle$,

$$\mathbf{d}_{fi} = \sum_{(k,l)} c_k^* c_l \langle \phi_k | \mathbf{r}_p | \phi_l \rangle \langle \chi_k | \chi_i \rangle, \tag{6.8}$$

where k and l are the indices over the components of the final and initial wave function, respectively.

We are now ready to estimate the total cross section using degenerate analysis of section 4.6. Our program uses a trial function of 320 components and 40 candidates per iteration, the overlap threshold was set at $T = 0.8$. Additionally we allow $\mathbf{a}$ to vary in all spherical directions. As we regard each spin state as equally likely in the ground state, we average the cross section over the three triplet states. The cross section is given in Figure 6.3.

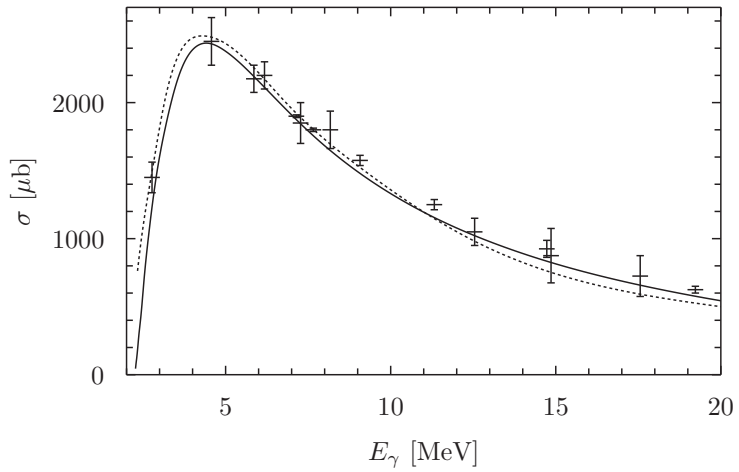

Figure 6.3: *Total cross section averaged over spin triplet states of the ground state (solid line). Experimental data and dotted line are the same as in* Figure 6.2.

Interestingly, in spite of the inclusion of spin dependent forces, the agreement with experiment diminishes slightly, rather than improving, by our modifications. The cause of this is not readily apparent, but a possible explanation is that we have only partially included the spin-dependent interaction in our model. The tensor term in the interaction was not taken into account. As it has the strength $V_T = -26.85$ MeV in the Garrido-Fedorov-Jensen potential, it can be assumed to have a noticeable effect on the p-wave states and

consequently the total cross section. In addition we note that higher orders of electromagnetic interaction and d-state admixture are not accounted for in our model, as described in section 6.1. Further studies are required to improve upon our model of the deuteron. Additional improvement of our model could be provided by including tensor forces, higher orders of electromagnetic interaction and d-state admixture. Such an undertaking is, however, beyond the scope of this thesis.

Chapter 7

Conclusions

In this thesis we have used the numerical method of correlated Gaussian functions to estimate the photodisintegration cross section of the deuteron.

We developed a variant of the correlated Gaussian functions with explicit p-wave nature and derived the analytic expressions to the necessary matrix elements. The efficacy of our p-wave basis was tested on the p-wave spectrum of hydrogen.

To examine the photodisintegration, we have derived the expressions of the cross section in the dipole approximation and considered correlated Gaussians in the quasicontinuum energy spectrum. We considered the deuteron bound state in the central force model and calculated the bound state and qausicontinuum states numerically where from the cross section of the deuteron photodisintegration was estimated. Through comparison with experiment we found that the quasicontinuum method satisfactorily produced the desired cross section for the deuteron photodisintegration. The quasicontinuum method with correlated Gaussians thus has the potential to describe more complicated systems and nuclear reactions involving continuum states.

Additionally we have made a first attempt at enhancing the quasicontinuum model by the inclusion of spin-dependent forces. The agreement with experiment were, however, diminished rather than improved by the inclusion. Further work is required to improve our model of the deuteron.

Bibliography

[1] Jensen, A.S., Siemens, P.J.: *Elements of Nuclei – Many-Body Physics with the Strong Interaction*, Addison-Wesley Publishing Company, Inc., 1987

[2] Ji, Xiangdong: *Nucleon-Nucleon Interaction, Deuteron* (lecture notes) `http://www.physics.umd.edu/courses/Phys741/xji/chapter6.pdf`

[3] Cobis, A., Jensen, A.S., Fedorov, D.V.: *The simplest "strange" three-body halo*, J.Phys. G 23, 401-421, 1997, arXiv:nucl-th/9608026

[4] Massachusetts Institute of Technology: *Neutron-Proton Scattering* (lecture notes), `http://mightylib.mit.edu/Course Materials/22.101/Fall 2004/Notes/Part3.pdf`

[5] Taasti, Vicki Trier and Nielsen, Lise Trier: *Store eksperimentelle øvelser: Deuteron photodisintegration*, IFA, Aarhus University, 2013

[6] Gasiorowicz, Stephen: *Quantum Physics*, 2nd Ed., John Wiley & Sons, Inc., 1996

[7] Bransden, B.H. and Joachain, C.J.: *Physics of Atoms and Molecules*, 2nd Ed., Pearson, 2003

[8] Rozpedzik, D. et al.: *Signatures of the chiral two-pion exchange electromagnetic currents in the 2H and 3He photodisintegration reactions*, Physical Review C 85:064004, 2011, arXiv:nucl-th/1103.4062v1

[9] Garrido, E., Fedorov, D.V. and Jensen, A.S.: *Three-body Halos. IV. Momentum Distributions after Fragmentation*, Physical Review, C 55:11327-1343, 1997, arXive:nucl-th/9608032v1

[10] Mitroy, Jim et al.: *Theory and application of explicitly correlated Gaussians*, Reviews of Modern Physics, vol. 85, 2013

[11] GNU project: *GNU Scientific Library Reference Manual: Cholesky Decomposition*, `https://www.gnu.org/software/gsl/manual/html_node/Cholesky-Decomposition.html`

[12] University of California, Berkeley: *Gram matrix*, `https://inst.eecs.berkeley.edu/~ee127a/book/login/def_Gram_matrix.html`

[13] Taasti, Vicki Trier: *Quantum states with high angular momentum in correlated Gaussian basis*, Bachelor's thesis, IFA, Aarhus University, 2012

[14] Griffiths, David: *Introduction to Quantum Mechanics*, 2nd Int. Ed., Pearson, 2005

[15] Partanen, T.M. and Niskanen, J.A.: *Parity nonconservation in deuteron photoreactions*, Eur. Phys. J., A 47:53, 2011, arXiv:nucl-th/1011.1807

Appendix A

Relevant matrix elements

In this appendix we derive the matrix elements used in our program to calculate the eigenenergies.

We begin with some relations that apply to all our derivations. Let $A > 0$ and $n = 0, 1, 2 \cdots$, we know

$$\int_{-\infty}^{\infty} x^{2n+1} \exp\left(-Ax^2\right) dx = 0, \tag{A.1}$$

because the integrand is an uneven function. Likewise

$$\int_{-\infty}^{\infty} x^{2n} \exp\left(-Ax^2\right) dx = 2\int_{0}^{\infty} x^{2n} \exp\left(-Ax^2\right) dx, \tag{A.2}$$

as the integrand is an even function. Further, according to Griffiths [14]

$$\int_{0}^{\infty} x^{2n} \exp\left(-Ax^2\right) dx = \sqrt{\pi}\frac{(2n)!}{n!}2^{-2n+1}A^{-n+\frac{1}{2}} \tag{A.3}$$

and

$$\int_{0}^{\infty} x^{2n+1} \exp\left(-Ax^2\right) dx = \frac{n!}{2}A^{-(n+1)}, \tag{A.4}$$

from which all our integrals can be derived via basic algebraic manipulations.

A.1 The s-wave matrix elements

We denote the s-wave basis functions

$$|A\rangle = \exp\left(-Ar^2\right). \tag{A.5}$$

The overlap matrix is given

$$\begin{aligned}\langle B|A\rangle &= \int_{-\infty}^{\infty}\int_{-\infty}^{\infty}\int_{-\infty}^{\infty} \exp\left(-(A+B)(x^2+y^2+z^2)\right) dxdydz \\ &= \left(\frac{\pi}{A+B}\right)^{3/2}.\end{aligned} \tag{A.6}$$

Similarly we derive the expectation value of the central potential,

$$\langle B|V_c(r)|A\rangle = V_c\left(\frac{\pi}{A+B+\frac{1}{b_c^2}}\right)^{3/2}. \tag{A.7}$$

We now wish to find the kinetic energy. The first thing we need is to apply the gradient,

$$\begin{aligned}\nabla|A\rangle &= \nabla\exp\left(-Ar^2\right)\\ &= -2A\exp\left(-Ar^2\right)\mathbf{r}.\end{aligned} \tag{A.8}$$

Next we apply the kinetic energy operator,

$$\begin{aligned}\langle B|\hat{T}|A\rangle &= -\frac{\hbar^2}{2\mu}\langle B|\nabla^2|A\rangle\\ &= -\frac{\hbar^2}{2\mu}\left(-\langle B|\nabla\right)\left(\nabla|A\rangle\right)\\ &= \frac{3}{\mu}\hbar^2 AB\pi^{3/2}(A+B)^{-5/2}.\end{aligned} \tag{A.9}$$

Additionally we are also interested in the root-mean-square radius of the deuteron. We remember that the radius is $\frac{1}{2}r$,

$$\frac{1}{4}\langle B|r^2|A\rangle = \frac{3}{8}\pi^{3/2}(A+B)^{-5/2}. \tag{A.10}$$

A.2 The p-wave and dipole moment matrix elements

We denote the p-wave basis functions

$$|a,A\rangle = \mathbf{a}\cdot\mathbf{r}\exp\left(-Ar^2\right). \tag{A.11}$$

The overlap matrix is given

$$\langle b,B|a,A\rangle = \mathbf{b}\cdot\mathbf{a}\frac{1}{2}\pi^{3/2}(A+B)^{-5/2}, \tag{A.12}$$

and the central potential element

$$\begin{aligned}&\langle b,B|V_c\exp\left\{-\frac{r^2}{b_{nn}^2}\right\}|a,A\rangle\\ &\quad= V_c\mathbf{b}\cdot\mathbf{a}\frac{1}{2}\pi^{3/2}\left(A+B+\frac{1}{b_{nn}^2}\right).\end{aligned} \tag{A.13}$$

We are also interested in the kinetic energy. We first apply the gradient operator,

$$\nabla|a,A\rangle = \left(\mathbf{a}-2A(\mathbf{a}\cdot\mathbf{r})\mathbf{r}\right)\exp\left(-Ar^2\right), \tag{A.14}$$

from which we derive the kinetic energy,

$$\langle b,B|\hat{T}|a,A\rangle = \frac{5}{2\mu}\hbar^2\pi^{3/2}\mathbf{b}\cdot\mathbf{a}AB(A+B)^{-7/2}. \tag{A.15}$$

The orbital angular momentum is also obtained,

$$\begin{aligned}\hat{L}|a,A\rangle &= -i\hbar\mathbf{r}\times\nabla|a,A\rangle \\ &= -i\hbar\mathbf{r}\times(\mathbf{a}-2A(\mathbf{a}\cdot\mathbf{r})\mathbf{r})\exp\left(-Ar^2\right) \\ &= -i\hbar\mathbf{r}\times\mathbf{a}\exp\left(-Ar^2\right), \end{aligned} \tag{A.16}$$

which yields

$$\langle b,B|L^2|a,A\rangle = \mathbf{b}\cdot\mathbf{a}\hbar^2\pi^{3/2}(A+B)^{-5/2}. \tag{A.17}$$

The harmonic oscillator potential has the matrix elements,

$$\langle b,B|\frac{1}{2}kr^2|a,A\rangle = \frac{5}{8}k\pi^{3/2}\mathbf{b}\cdot\mathbf{a}(A+B)^{-7/2}. \tag{A.18}$$

We now acquire the matrix elements of the spin-orbit potential. Assume that the state $|a,A\rangle$ is additionally assigned the spin $|\chi_a\rangle$,

$$\begin{aligned}&\langle\chi_b|\langle b,B|V_{\rm so}\hat{\mathbf{L}}\cdot\hat{\mathbf{S}}\exp\left\{-\frac{r^2}{b_{nn}^2}\right\}|a,A\rangle|\chi_a\rangle \\ &\quad= i\hbar V_{\rm so}\frac{1}{2}\pi^{3/2}(A+B+\frac{1}{b_{nn}})^{-5/2}(\mathbf{a}\times\mathbf{b})\cdot\langle\chi_b|\hat{S}|\chi_a\rangle, \end{aligned} \tag{A.19}$$

where $\langle\chi_b|\hat{S}|\chi_a\rangle$ is given in Table A.1.

Table A.1: *Expectation values of the inner product* $\langle\chi_b|\hat{S}|\chi_a\rangle$.

$\langle\chi_b\vert \quad\backslash\quad \vert\chi_a\rangle$	$\vert\uparrow\uparrow\rangle$	$\vert\downarrow\downarrow\rangle$	$\frac{1}{\sqrt{2}}(\vert\uparrow\downarrow\rangle+\vert\downarrow\uparrow\rangle)$	$\frac{1}{\sqrt{2}}(\vert\uparrow\downarrow\rangle-\vert\downarrow\uparrow\rangle)$
$\langle\uparrow\uparrow\vert$	(0,0,1)	(0,0,0)	$\frac{1}{\sqrt{2}}(1,-i,0)$	(0,0,0)
$\langle\downarrow\downarrow\vert$	(0,0,0)	(0,0,-1)	$\frac{1}{\sqrt{2}}(1,i,0)$	(0,0,0)
$\frac{1}{\sqrt{2}}(\langle\uparrow\downarrow\vert+\langle\downarrow\uparrow\vert)$	$\frac{1}{\sqrt{2}}(1,i,0)$	$\frac{1}{\sqrt{2}}(1,-i,0)$	(0,0,0)	(0,0,0)
$\frac{1}{\sqrt{2}}(\langle\uparrow\downarrow\vert-\langle\downarrow\uparrow\vert)$	(0,0,0)	(0,0,0)	(0,0,0)	(0,0,0)

Next we are interested in the spin-spin interaction,

$$\begin{aligned}&\langle\chi_b|\langle b,B|V_{ss}\mathbf{s}_1\cdot\mathbf{s}_2\exp\left\{-\frac{r^2}{b_{nn}^2}\right\}|a,A\rangle|\chi_a\rangle \\ &\quad= \langle\chi_b|\mathbf{s}_1\cdot\mathbf{s}_2|\chi_a\rangle V_{ss}\mathbf{b}\cdot\mathbf{a}\frac{1}{2}\pi^{3/2}\left(A+B+\frac{1}{b_{nn}^2}\right), \end{aligned} \tag{A.20}$$

where $\langle\chi_b|\mathbf{s}_1\cdot\mathbf{s}_2|\chi_a\rangle$ is given in Table A.2.

We also need the matrix element from the Coulomb potential,

$$\langle b,B|\frac{-1}{r}|a,A\rangle = -\mathbf{b}\cdot\mathbf{a}\int_{-\infty}^{\infty}\int_{-\infty}^{\infty}\int_{-\infty}^{\infty}\frac{z^2}{r}\exp\left(-(A+B)r^2\right)dxdydz. \tag{A.21}$$

The above integral is straightforward to solve in spherical coordinates,

$$\langle b,B|\frac{-1}{r}|a,A\rangle = -\mathbf{b}\cdot\mathbf{a}\frac{2}{3}\pi(A+B)^{-2}. \tag{A.22}$$

Table A.2: *Expectation values of the innerproduct* $\langle\chi_b|\mathbf{s}_1\cdot\mathbf{s}_2|\chi_a\rangle$.

$\langle\chi_b\vert \quad \backslash \quad \vert\chi_a\rangle$	$\vert\uparrow\uparrow\rangle$	$\vert\downarrow\downarrow\rangle$	$\frac{1}{\sqrt{2}}(\vert\uparrow\downarrow\rangle+\vert\downarrow\uparrow\rangle)$	$\frac{1}{\sqrt{2}}(\vert\uparrow\downarrow\rangle-\vert\downarrow\uparrow\rangle)$
$\langle\uparrow\uparrow\vert$	1	0	0	0
$\langle\downarrow\downarrow\vert$	0	1	0	0
$\frac{1}{\sqrt{2}}(\langle\uparrow\downarrow\vert+\langle\downarrow\uparrow\vert)$	0	0	1	0
$\frac{1}{\sqrt{2}}(\langle\uparrow\downarrow\vert-\langle\downarrow\uparrow\vert)$	0	0	0	-1

Lastly, we are interested in the dipole moment, $\mathbf{d}_{fi}$, where each element is given

$$\begin{aligned}\langle b,B|\mathbf{r}_p|A\rangle &= \langle b,B|\frac{1}{2}\mathbf{r}|A\rangle \\ &= \frac{1}{2}\pi^{3/2}(A+B)^{-5/2}\mathbf{b}. \end{aligned} \tag{A.23}$$